European Review for Medical and Pharmacological Sciences 2020; 24: 4909-4920

Hypoxia factors suppression effect on the energy metabolism of a malignant melanoma cell SK-MEL-30

I. ŠPAKOVÁ[1], W.F. GRAIER[2,3], M. RABAJDOVÁ[1], K. DUBAYOVÁ[1], V. NAGYOVÁ[4], M. MAREKOVÁ[1]

[1]Department of Medical and Clinical Biochemistry, Pavol Jozef Šafárik University in Košice, Faculty of Medicine, Košice, Slovakia
[2]Gottfried Schatz Research Center, Molecular Biology and Biochemistry, Medical University of Graz, Graz, Austria
[3]BioTechMed, Graz, Austria; [4]Department of Dermatovenerology, Pavol Jozef Šafárik University in Košice, Faculty of Medicine, Košice, Slovakia

Abstract. – OBJECTIVE: Malignant melanoma (MM), as well as other cancers, is a disorder in the cell life cycle at many levels. In terms of energy, the sync of cytosolic and mitochondrial metabolism is required for each cell. Mismatches also caused by hypoxic factors accumulate defects leading to the formation, development and invasiveness of malignant melanoma. Our aim was to compare the effect of HIF-1α and miR-210 on the metabolism of malignant melanoma cells in normoxia and pseudohypoxia. Further, we also investigated how gene silencing affects the viability in order to evaluate the potential of gene therapy in the treatment of MM.

MATERIALS AND METHODS: We targeted oxidative phosphorylation by genetically suppressing HIF-1α and miR-210. We have examined mitochondrial activity, cytosolic glycolysis and cell viability.

RESULTS: The ratio of NADH/NAD$^+$ in the cytoplasm under normal conditions is stable and can thus serve as a specific cellular metabolic marker. Therefore, the study was aimed at finding the cause of the reduction in NADH levels in increasing hypoxia under ideal *in vitro* conditions on the SK-MEL-30 malignant melanoma cells. The relationship between HIF-1α and miR-210, their effect on transcriptional level, and the subsequent effect on metabolic process attenuation in cells was investigated. Obtained results indicate that the NADH which is accumulated by cells in hypoxia was significantly decreased upon gene silencing.

CONCLUSIONS: Our studies have shown that small regulatory molecules with organelle-specific effect (such as miRs) need to be targeted, and that the resultant effect is comparable to silencing of "general" hypoxic transcription factors.

Key Words:
Malignant melanoma, Mimic hypoxia, NADH, HIF-1α, MiR-210.

Introduction

Cells under physiological conditions gain energy for all vital functions by combining cytosolic and mitochondrial metabolism. The main substrate glucose (Glc) is metabolised to pyruvate in glycolytic pathway in cytoplasm which is subsequently followed by citric acid cycle (TCA) and oxidative phosphorylation (OXPHOS) in mitochondria to produce adenosine triphosphate (ATP). This process responds sensitively to the changes in oxygen concentration in the cell and, if it is deficient (hypoxia), the protection mechanisms are triggered in the cell and, in order to survive, the cell energy is only obtained in cytosol (as kinetically more favourable process). When the optimum oxygen concentration is restored, mitochondria are involved in ATP formation again. Cancer cells (e.g., melanomas) often undertake activation of processes such as in oxygen deficiency under normal oxygen conditions (pseudohypoxia), and the aerobic glycolysis behaves as an anaerobic pathway producing lactate and is disconnected from the citric acid cycle and OXPHOS. This action is well known as the Warburg effect[1], which is characterized by the accumulation of lactate, NADH (reduced nicotinamide

Corresponding Author: Ivana Špaková, MD; e-mail: spakovaivana@gmail.com
ivana.spakova@upjs.sk

adenine dinucleotide) and an increase of hypoxic transcription factors (HTFs).

Orientation of energy metabolism only to the cytosol in cancer cells hinders the transport of NADH from glycolysis and other metabolic processes from cytosol to mitochondria. Therefore, NADH, as an energy substrate in OXPHOS, accumulates in the cytoplasm of a malignant cells[2].

The most studied HTFs are hypoxia-inducible factors (HIF-1,2,3 and their α/β heterodimers) which activate oxygen homeostasis disruption adaptation genes[3]. Healthy cells in hypoxia will increase transcription of HIFs (e.g., HIF-1α) which activates a number of additional supporting genes. Upon returning to the state of optimum oxygen concentration HIF-1α is prolyl-hydroxylated by PHD (prolyl 4-hydroxylase) and binding with Rbx1 (Ring-Box 1), VHL (Von Hippel-Lindau), ubiquitin is ultimately inactivated via proteasome degradation[4]. Melanoma cells do not subject HIF-1α degradation in proteasome due mutations in regulatory genes (microphthalmia-associated transcription factor – MITF, glioma-associated family of transcription factors – GLI, prolyl hydroxylase – PHD, etc.) and thus the influence of the oncogenic HIF-signalling pathway increases. This HIF-signalling pathway positively affects glucose metabolism-modulating enzymes and negatively affects in mitochondrial enzymes.

HIF-pathway regulates induction of hypoxia micro-RNAs (hypoxamiRNAs) (including miR-210, -373, -103 etc.)[5]. MiR-210, one of the most studied hypoxamiRNA, is activated via stabilisation of HIF-1α[6]. Its main role is disconnection of electron transport in respiratory complex I (repressing iron-sulphur cluster assembly enzyme – ISCU, cytochrome c oxidase assembly 10 – COX10)[7,8]. Silencing of miR-210 has a beneficial effect on mitochondrial oxidative metabolism and attenuate proliferation and glycolytic activity[9]. HIF-1α and miR-210 have positive feedback regulatory system, decreased expression of HIF-1α results in simultaneous decrease of miR-210 expression, and *vice versa*[7,10]. However, expression of miR-210 also depends on expression of other HIFs which causes the decrease of miR-210 expression to be less evident[10]. The phenomenon known as HIF switch during chronic hypoxia is regulated by miR-210 (and other hypoxamiRs) and could explain the curious effect when downregulation of one type of HIF evoke increase of other HIF[11]. It was observed that miR-210 is overexpressed in the late stages of cancer[10,12-14] and leads to poor prognosis of a disease.

In normoxia, pyruvate is transported to the mitochondria where the pyruvate dehydrogenase complex (PDC) is converted to Acetyl-CoA. *Pyruvate dehydrogenase A1* (PDHA1) is part of the pyruvate dehydrogenase complex, and its activity is regulated by PDK1 (pyruvate dehydrogenase kinase)[15]. PDHA1 inhibits the progression of cancer by affecting fatty acid biosynthesis. Inactivation of PDHA1 (e.g., by serine phosphorylation, Ser-293, and tyrosine phosphorylation, Tyr-301) affects NADH active site accessibility, regulates PDC secondary activity, and supports the Warburg effect[15].

Hypoxia-induced factor HIF-1α inhibits PDHA1 by activation of PDK1 (*pyruvate dehydrogenase kinase 1*), thereby preventing both pyruvate and NADH from flowing into mitochondria. Thus, NADH remains "trapped" in the cytosol[16,17].

The mitochondrial membrane is porous and freely permeable to the inner membrane space for the NADH molecule. On the inner mitochondrial membrane NADH is transported by the malate-aspartate or glycerol-3-phosphate shuttle. Consequently, the cytoplasmic NADH level may affect the alteration of the mitochondrial NADH/NAD^+ ratio[18]. Based on this communication of cytosolic and mitochondrial metabolism it is possible to determine respiration efficiency under normo- and hypoxic conditions in order to describe overall metabolic state of the cell.

Cancer cells often use glutaminolysis as compensation of glycolysis[19]. Glutamine (Gln), one of the most represent plasma protein, can be used as energy source thought anaplerotic conversion to 2-oxoglutarate (2OG) in citric acid cycle[20]. Highly proliferative cancer cells use this pathway to rehabilitate NADH to NAD^+[21] and produce energy (6 ATP)[22]. 2OG can be also converted to citrate by isocitrate dehydrogenase and simultaneously NADH is rehabilitated in a reverse pathway named reductive carboxylation[23,24]. Gln is involved in de novo synthesis of cholesterol and fatty acids. Fatty acids and glutamate are immunosuppressive and their amount increases with stage of the disease[25,26].

In this study, we focused on monitoring of pro-cytosolic processes activation using the ratio of free cytosolic NADH/NAD^+ while its disruption by NADH increase can be used as a cancer metabolic marker[27,28]. In our work, we tried to find a regulatory gene which upon activation or inactivation would restore the cooperation of cytosolic and mitochondrial metabolism and thus prevent the malignant cell from surviving and multiplying. Therefore, we decided to compare the effect of gene silencing of "general" hypoxic factor HIF-1α with the gene silencing of miR-210 in MM cells fed with glucose or glutamine, respectively.

Materials and Methods

Materials

Dulbecco's Modified Eagle's Medium (DMEM) Culture Medium (Thermo Fisher Scientific, Waltham, MA, USA), Fetal Calf Serum (FCS; Thermo Fisher Scientific, Waltham, MA, USA), Phosphate-Buffered Saline (PBS; Thermo Fisher Scientific, Waltham, MA, USA), 0.25% Trypsin (Thermo Fisher Scientific, Waltham, MA, USA), TransFast™ Transfection Reagent (Promega, Madison, WI, USA), small interfering RNA (siRNA) HIF-1α (Oligo ID# 2808643) (Microsynth AG, Balgach, Switzerland), siRNA miR210 (Oligo ID# 2808645) (Microsynth AG, Balgach, Switzerland), $CoCl_2 \cdot 6H_2O$ (Sigma-Aldrich, St. Louis, MO, USA), Glutamine (Thermo Fisher Scientific, Waltham, MA, USA), Pyruvate (Sigma-Aldrich, St. Louis, MO, USA), Lactate (Sigma-Aldrich, St. Louis, MO, USA), Glucose monohydrate (Sigma-Aldrich, St. Louis, MO, USA), $CaCl_2$ (Sigma-Aldrich, St. Louis, MO, USA), NaCl (Sigma-Aldrich, St. Louis, MO, USA), $MgCl_2$ (Sigma-Aldrich, St. Louis, MO, USA), KCl (Sigma-Aldrich, St. Louis, MO, USA), Hepes (Sigma-Aldrich, St. Louis, MO, USA), 0.4% Tryptan Blue (Thermo Fisher Scientific, Waltham, MA, USA), SeaHorse Assay medium (SeaHorse Bioscience, North Billerica, MA, USA), SeaHorse hydration medium (SeaHorse Bioscience, North Billerica, MA, USA), Elastohydrodynamic Lubrication (EHL; Thermo Fisher Scientific, Waltham, MA, USA), Antimycin A (Sigma-Aldrich, St. Louis, MO, USA), Oligomycin (Sigma-Aldrich, St. Louis, MO, USA), FCCP (Sigma-Aldrich, St. Louis, MO, USA), pcDNA3.1-Peredox-mCherry (plasmid 32383) (Addgene, Watertown, MA, USA).

Molecular Analysis

Changes in the expression level of mRNA for HIF-1α, PDHA1, and the housekeeping gene glyceraldehyde-3-phosphate dehydrogenase (GAPDH) in the SK-MEL-30 cell suspension were detected. The expression of the miR-210, and miR-housekeeping gene U6 in the SK-MEL-30 cell suspension were determined. The sequences of used reverse and forward primers are shown in Table I.

The acquired RNA samples were transcribed by reverse PCR into cDNA using specific reverse primers individually for HIF-1α (L6237B06, resp. B07) (Thermo Fisher Scientific, Waltham, MA, USA), PDHA1 (R0443A07, resp. A08) (Thermo Fisher Scientific, Waltham, MA, USA), GAPDH (Thermo Fisher Scientific, Waltham, MA, USA), miR-210 (L6237B02, resp. B03) (Thermo Fisher Scientific, Waltham, MA, USA) and U6 (L6237B04, resp. B05) (Thermo Fisher Scientific, Waltham, MA, USA) using the Total RNA kit peqGOLD (Peqlab Biotechnologie GmbH, Erlangen, Germany) and the microRNA Purification Kit (Norgen Biotek Corp., Thorold, Ontario, Canada). The RNA samples were transcribed to cDNA using the High-Capacity cDNA Reverse Transcription Kit (Applied Biosystems, Foster City, CA, USA). The cDNA samples were amplified using the GoTaq qPCR Master Mix (Promega, Madison, WI, USA) 40 cycles (95°C/5 min, 95°C/15 s, 58-62°C/20 s, and 72°C/25 s) protocol using the corresponding specific primer sequences. LightCycler 480 Instrument II (Hoffmann-La Roche, Basel, Switzerland) was used for RT-PCR analysis. Due to the biological variability of the biological material samples, the analysed samples were measured in triplicate for each gene of interest. Changes in mRNA expression for the genes of interest (HIF-1α, PDHA1, miR-210) were evaluated by comparative quantification and Ct values using the GraphPad Prism version 5.04 software.

Cell Line and Cultivation Conditions

Expression levels of selected genes in microenvironmental normoxia or hypoxia (mimic hypoxia) were detected *in vitro* in the SK-MEL-30 malignant melanoma cell line (Cell Bank Graz, Medical University of Graz, Austria). The expres-

Table I. Gene F/R sequences.

Gene	Forward (sense) sequenceReverse (antisense) sequence
GAPDH	TGGGGCCAAAAGCATCATCTCGCCGCCTGCTTCACCACCTTCTT
HIF-1α	CGTTCCTTCGATCAGTTGTCTCAGTGGTGGCAGTGGTAGT
PDHA1	ATGTGGAAGTGAGGAAGGAGTCGCTGGAGTAGATGTGGTA
miR-210	CTGTGCGTGTGACAGGTGCAGGGTCCGAGGT
U6	CTCGCTTCGGCAGCACAAACGCTTCACG AATTTGCGT

sion of genes involved in the oncological transformation of HIF-1α cells, miR-210, and genes for gene-linking of cytosolic and mitochondrial metabolism, such as PDHA1, were studied. The metabolic status of the SK-MEL-30 cell line was monitored by the development of NADH, ATP levels, and mitochondrial respiration efficiency at different oxygen conditions in the cells.

Normoxic culture conditions were adjusted by culturing SK-MEL-30 cells in DMEM culture medium containing 10% FCS, 100 U/ml penicillin, 100 µg/ml streptomycin and 2 mM glutamine, respectively, in a thermo-incubator at 37°C and a 5% CO_2 atmosphere. Hypoxic conditions were induced by the addition of 100 µM $CoCl_2 \cdot 6H_2O$ to the culture medium which mimics hypoxia in the cell, thereby activating metabolic pathways characteristic of oxygen deficiency[29].

To monitor NADH and ATP metabolism, cells were seeded on 30 mm slides and briefly transfected at 60-80% confluency with 100 µM siRNA encoding the mCherry PEREDOX biosensor with 2.5 µl TransFast™ transfection solution for 12-16 hours. After transfection the culture medium was changed with an emphasis on maintaining normo- or hypoxic conditions. The experiments were performed within 48 hours of transfection using siRNAs, mCherry PEREDOX.

Experimental measurements of NADH were performed using a flow system with manual control of additive circulating media based on Ca^{2+}/Na^+ phosphate buffer, pH = 7.4, 10 mM glucose, 10 mM pyruvate, 10 mM lactate or 10 mM glutamine, respectively, 100 µM $CoCl_2 \cdot 6H_2O$; solutions were added systematically to the base Ca^{2+}/Na^+ phosphate medium.

siRNA and Transfection

Transfected siRNA with the sequence for HIF-1α: 5'-CCA CCA CUG AUG AAU UAA AUU TT-3' and for miR-210: 5'-UCA GCC GCU GUC ACA CGC ACA GTT-3'. Selected siRNAs were applied to the affected cells by reverse transfection using the Transfast™ Transfection Reagent technology. To analyse transfection efficiency (by RT-PCR), cells were transfected using Transfast™ without siRNA and the presented negative treatment control (NTC). Cells were transfected overnight (12 hours).

Peredox Assay

PEREDOX-mCherry analysis is based on the genetically encoded fluorescent biosensor formed by the florescence-labelled Rex-cpFP complex[30] which is activated upon the binding of the NADH molecule. Binding of the reduced NADH molecule will increase the fluorescence intensity of the complex. The reaction is reversible and removal of the NADH molecule does not result in more fluorescence. Real-time production of the relative cytosolic NADH/NAD^+ level in SK-MEL-30 cells was detected using Nikon Eclipse Till-imaging Fluorescence-Optical Technology (Till Photonics, Gräfelfing, Germany) with a specimen motion stand, polychrome V (Till Photonics, Gräfelfing, Germany) and a 40x/1.3 oil lens (Alpha Plan Fluar 40x, Zeiss, Göttingen, Germany). A NADH genetically encoded ratiometric fluorescent indicator biosensor, PEREDOX-mCherry, was emitted at two wavelengths: 430 nm (green) and 570 nm (red). Fluorescence 430/570 (green/red) represents the NADH/NAD^+ ratio and calculated as: Δ max Ratio, where R_0 is normalised amplitude. Individually measured cells were adjusted to the background brightness and the so-called green-to-red share was evaluated using the Live Acquisition 2.0.0.12 software (Till Photonics, Gräfelfing, Germany).

Seahorse XF96

Mitochondrial viability was measured under normoxic and hypoxic conditions using the Seahorse XF96 technology. The oxygen tension-dependent mitochondrial activity was measured for input energy substrates of 10 mM glucose and 10 mM glutamine. The measured respiratory activities of the cancer microenvironment were analysed for oxygen consumption rate (OCR), which describes mitochondrial respiration and mitochondria generating ATP. In resting cell mode, ATP synthesis and consumption are balanced. Changes in the OCR reflect changes in ATP production which correspond to changes in cell ATP consumption.

Statistical Analysis

Mean Ct values (threshold cycle) and standard deviations depended on a relative concentration of the target are used in the ΔCt calculations. The variance of the ΔCt is calculated from the standard deviations of the target and reference values (calibrator). The result is a multiple of the calibrator concentration. The obtained data were analysed with GraphPad Prism version 5.04 (La Jolla, CA, USA). The presented data are mean ± standard error of mean (SEM) in 5 independent experimental repeats. The

two-tailed Student's *t*-test was used to compare the data obtained in the two groups. When comparing values among multiple groups, the one-way ANOVA statistical method was used to evaluate statistical significance, more specifically Tukey's Multiple Comparison test. Statistically significant results were found to have a *p*-value between 0.01 and 0.05 indicated by "*", a *p*-value between 0.001 and 0.01 with indicated by "**", a *p*-value is less than 0.001 indicated by "***".

Results

Cell Redox State Depends of Cytosolic NADH Level

Under normoxic conditions, we determined the NADH/NAD$^+$ ratios (Figure 1-A) of cells saturated with 10 mM glucose to ± 100% (the NADH/NAD$^+$ ratio in normoxia for unaffected cells was chosen as the baseline; NADH/NAD$^+$ = lactate/pyruvate ratio) and glutamine ± 11% ($p < 0.001$), taken to glucose (Figure 1-B-1, 2). Cells

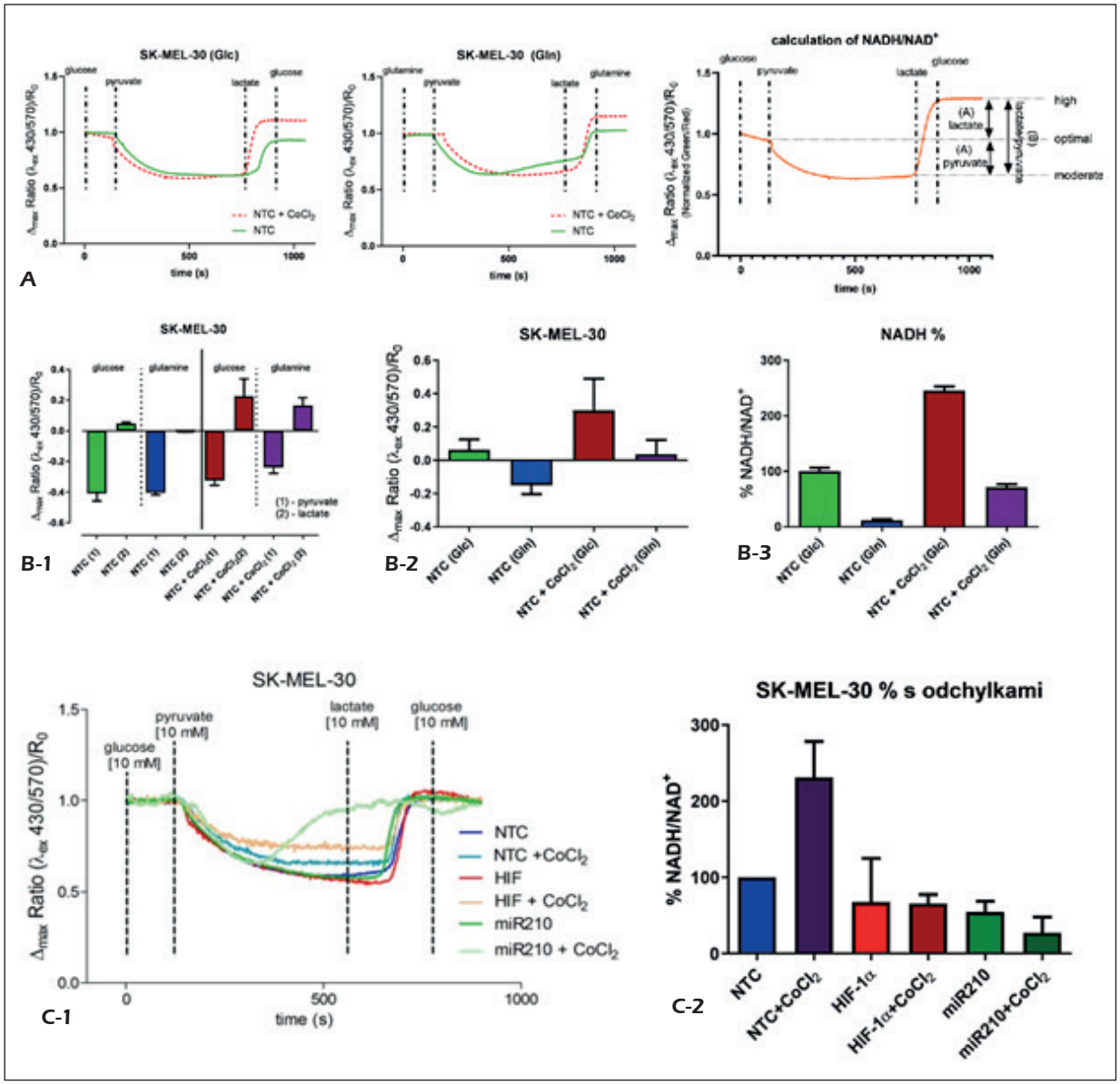

Figure 1. A, Detection of changes in the NADH/NAD+ ratio using PEREDOX-mCherry Assay; **B**, The calculated NADH/NAD+ ratio produced by cells consuming glucose (Glc) or glutamine (Gln): (1) – mean of the decrease in the NADH/NAD+ ratio, (2) – the difference in the NADH/NAD+ ratio from the lactate/pyruvate, (3) – percentage of NADH from the difference of the NADH/NAD+ ratio; **C**, NADH/NAD+ ratio produced by cells after Glc consumption in HIF-1α or miR-210 gene silencing.

saturated with 10 mM glutamine instead of glucose were presented with a significantly lower NADH production of ± 71% ($p < 0.001$) under hypoxic conditions *vs.* 10 mM glucose-fed cells where a mean of ± 245% ($p < 0.001$) was measured (Figure 1-B-3).

The ratio of NADH/NAD^+ in normoxia for the uninfluenced cells was chosen as the baseline; it is 100% (Figure 1-C-1, 2). In hypoxia the NADH/NAD^+ ratio increased to ± 231% ($p < 0.001$). After HIF-1α gene silencing the produced NADH/NAD^+ ratio decreased to ± 67% in normoxia, and to ± 65% in hypoxia ($p < 0.01$). The effect of miR-210 gene silencing in normoxia was a decrease in the NADH/NAD^+ ratio to ± 54% ($p < 0.01$), and in hypoxia to ± 27% ($p < 0.01$).

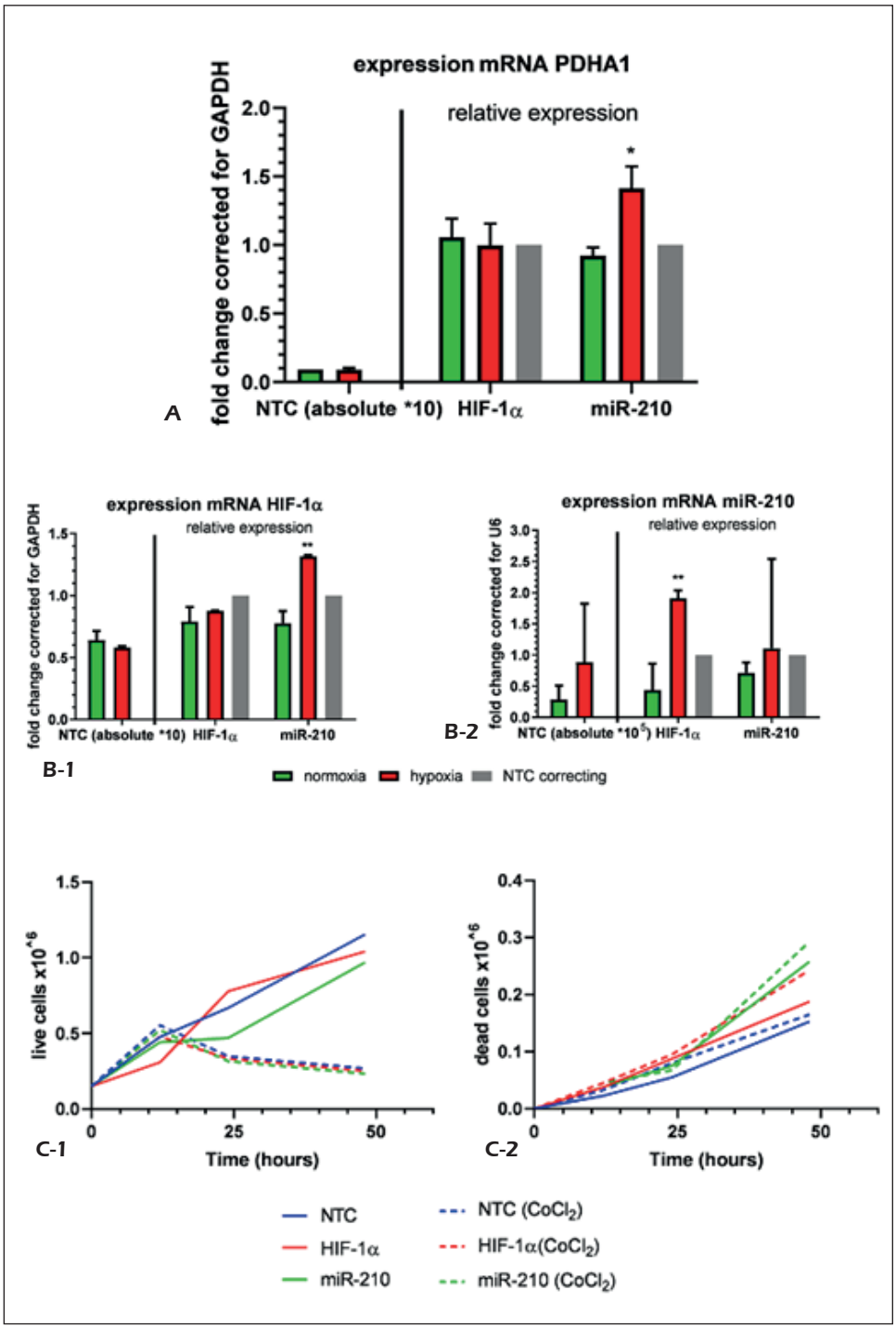

Figure 2. **A**, Relative expression of mRNA PDHA1 gene; **B**, Relative expression of mRNA to NTC normoxia/hypoxia: (1) – HIF-1α gene expression, (2) – miR-210 gene; **C**, Cell growth line of SK-MEL-30 (1) and number of apoptotic cells SK-MEL-30 (2).

Expression of PDHA1

The level of PDHA1 absolute gene expression (Figure 2-A) in normoxia of NTC was 0.009; the relative expression of PDHA1 was 1.057 in HIF-1α expression-suppressed cells, and 0.922 in miR-210 expression-suppressed cells. No statistically significant differences were detected when comparing different cell groups under normoxic conditions.

The level of relative expression of the gene of interest in NTC determined in hypoxia was 0.00916. In cells with HIF-1α gene silencing the relative expression of PDHA1 was 0.998, and in the cells with miR-210 gene silencing it was 1.415. The difference between expression in normo- and hypoxic conditions in cells affected by miR-210 gene silencing was at a $p < 0.05$ significance level.

Detection of HIF-1α and MiRNA-210 Expression Level

Cells in the NTC control group (0.887015) had a higher expression of miR-210 than miR-210 silenced cells (0.713144) in normoxia. Cells with HIF-1α gene silencing (1.9138315) were characterised by the highest level of miR-210 expression (Figure 2-B).

The level of relative expression of HIF-1α in normoxia in NTC control cells was 0.05945; in cells with HIF-1α attenuation it was 0.05043, and in cells with miR-210 silencing expression suppression it was 0.05013. The measured level of relative expression of the gene of interest in hypoxia was 0.05357 in NTC cells, 0.05484 in HIF-1α-attenuated cells and 0.07489 in cells with miR-210 expression suppressed. We determined the significance of the expression of HIF-1α mRNA by NTC cells and after the silencing of miR-210 expression at $p < 0.01$ under hypoxic conditions, as well as by comparing HIF-1α mRNA expression between cells with targeted suppression of miR-210 silenced expression at $p < 0.01$.

Cell Viability in Normo- and Hypoxic Conditions

We analysed cell growth under normoxic and hypoxic conditions and evaluated how many cells were subject to apoptosis after 48 hours of incubation with/without 100 μM $CoCl_2 \cdot 6H_2O$ (Figure 2-C).

We observed that after 12 hours of growth cells reached a stationary phase under hypoxic conditions (Figure 2-C-1), while cells under normoxic conditions reached a stationary phase after 80-90 hours of culturing. The significance level was $p < 0.05$ in living cells counted in normoxia at 48 hours of culture in siRNA-treated HIF-1α cells *vs*. control of NTC and miR-210 siRNA at $p < 0.01$. In hypoxia, a nonsignificant change in the number of viable cells was observed compared to the NTC control group.

The measured values indicate only a minimal increase in dead cells in the negative control under hypoxic conditions. The most pronounced apoptotic behaviour was observed in the miR-210 transfected cells in both normoxic and hypoxic conditions. The significance level was at $p < 0.05$ in the number of apoptotic/dead cells in normoxia in a comparison of NTC to cells with HIF-1α silencing expression, and miR-210 was at a significance level of $p < 0.01$ (Figure 2-C-2). In hypoxia, a level of significance at $p < 0.01$ was observed in HIF-1α expression-inhibited cells and at $p < 0.001$ for cells with miR-210 expression suppressed.

Mitochondrial Redox State Represents the Level of ATP Production

An average level 14.14 pMol/min in the basal respiration (BR) was observed in normoxia and 19.00 pMol/min in hypoxia for NTC glucose-fed cells (Glc) (Figure 3-A-1, Table II). Gene silencing of HIF-1α + Glc of analysed cells resulted in an increase of basal respiration level up to 52.14 pMol/min in normoxia, and 63.57 pMol/min in hypoxia. Likewise, gene silencing of miR-210 + Glc resulted in an increased of BR level up to 30.14 pMol/min in normoxia, and 40.29 pMol/min in hypoxia. Significant changes were observed at $p < 0.01$ upon comparing basal respiration. Significant changes were observed at $p < 0.001$ upon comparing MCR of analysed cells (Figure 3-B-1, Table II).

We observed in the BR average level 18.00 pMol/min in normoxia, and 18.43 pMol/min in hypoxia of NTC glutamine-fed cells (Gln) (Figure 3-A-2, Table II). Gene silencing of HIF-1α + Gln of analysed cells resulted in an increase of basal respiration level up to 56.43 pMol/min in normoxia, and 57.14 pMol/min in hypoxia. Likewise, gene silencing of miR-210 + Gln resulted in an increased of BR level up to 47.71 pMol/min in normoxia, and 69.43 pMol/min in hypoxia (Figure 3-B-2, Table II).

Discussion

Cancer cells often use only cytosolic metabolism (anaerobic glycolysis), although there is a

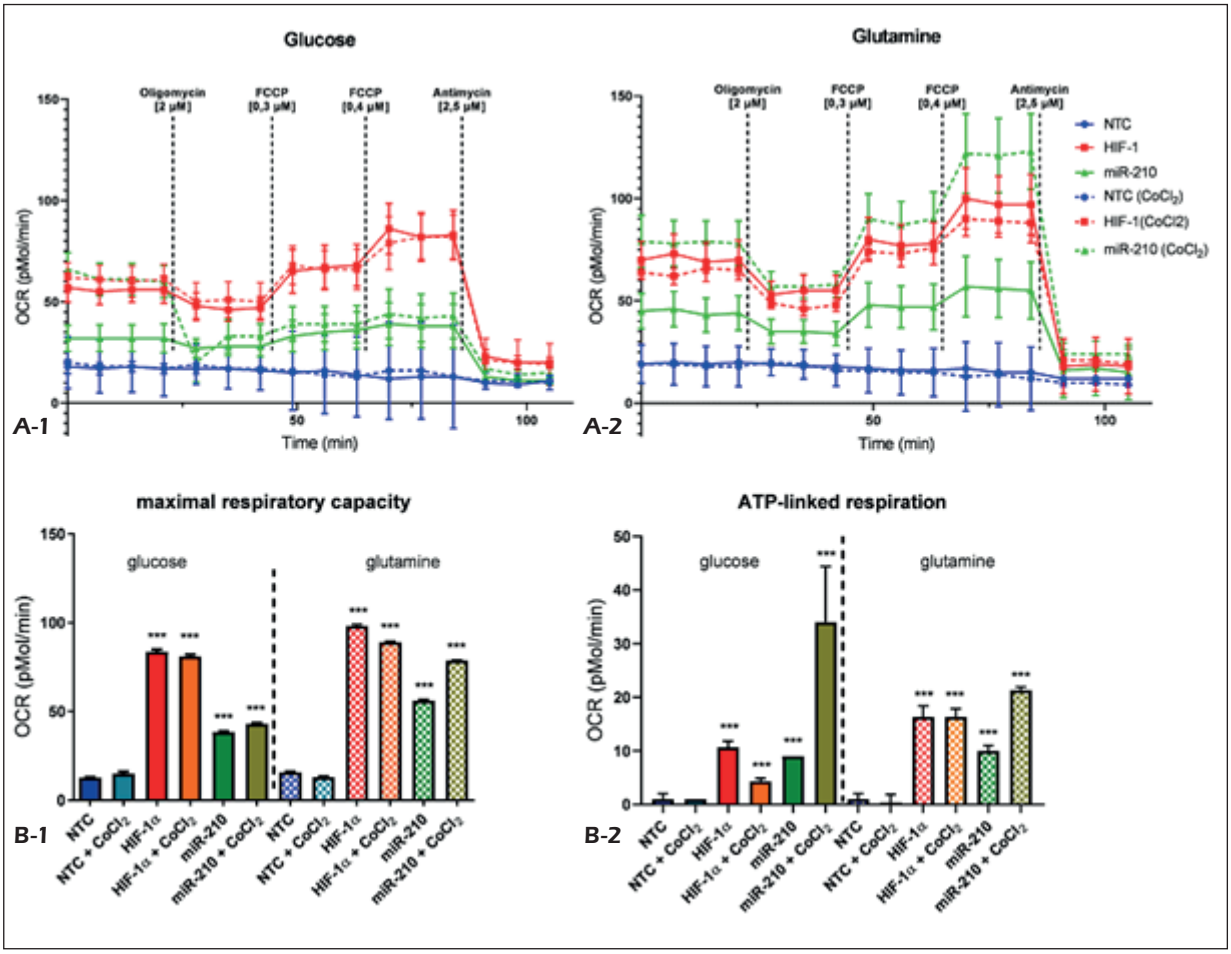

Figure 3. A, OCR of SK-MEL-30. (1) – cells cultured with 10 mM glucose (Glc), (2) – cells cultured with 10 mM glutamine (Gln); **B**, Maximal respiratory capacity and ATP-linked respiration (based on Seahorse).

group of cells that are characterised by indeterminate metabolism and occasionally use oxidative phosphorylation to form ATP[31]. Cancer cells also accumulate lactate during mimic hypoxia, the concentration of which correlates with the aggressiveness of the tumour disease[32]. Based on the Warburg theory, NADH also accumulates in the cytosol of cancer cells along with lactate reflecting the degree of disease in similar manner.

Cell Redox State Depending on Cytosolic NADH Level

Cellular redox status, derived from the primary production of NADH and expressed as the ratio of NADH/NAD^+ levels in the cytosol of cells, can be detected by Peredox-mCherry live cell imaging[30]. In the experiment the baseline level of NADH in the cytosol of cells was determined at 10 mM glucose in circulating buffer solution. The NADH/NAD^+ ratio decreased after the addition of 10 mM pyruvate to Ca^{2+}/Na^+ buffer solution until cell metabolism was stabilised. Subsequently, the cells were saturated with Ca^{2+}/Na^+ buffer solution with 10 mM lactate and the accumulation of NADH was monitored until its production was stabilised (Figure 1-A). The difference between the NADH/NAD^+ ratio after the addition of pyruvate and lactate was calculated as the relative amount of NADH in the cytosol of the cells.

However, in hypoxia with Gln cells (cells cultivated with 10mM of Glutamine) the NADH/NAD^+ ratio is in favour of NAD^+ which correlates with measurements in patients where a decrease in circulating NADH in hypoxia was observed (i.e., cancer and its increasing stage)[33]. The result is consistent with glutamine metabolism *via* reductive carboxylation due to decreased NADH utilisation in mitochondria. Cells affected by HIF-1α siRNA or miR-210 siRNA produced significantly less NADH in both normoxia and hypoxia (Figure 1-C-1, 2).

Table II. Levels of OCR of basal respiration, proton leak, maximal respiration capacity and ATP in measured conditions of SK-MEL-30.

	Glucose		Glutamine	
	Normoxia	Hypoxia	Normoxia	Hypoxia
Basal respiration (pMol/min)				
NTC	14.14	19.00	18.00	18.43
HIF-1α	52.14	63.57	56.43	57.14
miR-210	30.14	40.29	47.71	69.43
Proton leak (pMol/min)				
NTC	16.67	17.67	18.33	18.33
HIF-1α	47.00	50.33	54.33	47.67
miR-210	27.67	28.67	34.67	57.33
Maximal respiratory capacity (pMol/min)				
NTC	14.00	16.33	14.40	15.33
HIF-1α	73.60	78.33	72.20	74.33
miR-210	36.20	47.33	41.40	89.00
ATP-linked respiration (pMol/min)				
NTC	1.00	1.00	1.00	0.33
HIF-1α	10.67	4.33	16.33	16.33
miR-210	9.00	34.00	10.00	21.33

Expression of PDHA1

HIF-1α or miR210 silencing in normoxia does not affect PDHA1 expression. Thus, the transfer of pyruvate to the mitochondrial matrix is identical in all cases – even in hypoxia. SK-MEL-30 malignant melanoma cells are characterised by a preference of cytosolic metabolism. The reduced effect of HIF-1α by silencing reduces PDK1 activity and thereby activates PDHA1 (dephosphorylates). Since PDHA1 is regulated via miR-210, the silencing of miR-210 is adequately induced by upregulation of electron transfer proteins, such as PDHA1 (Figure 2-A)[34] or the ISCU1/2 (iron-sulphur cluster assembly proteins 1/2, of respiratory complexes I and III)[17]. More NADH molecules are transferred to the mitochondria and do not accumulate in the cytosol of the cell. The difference between expression in normo- and hypoxic conditions in cells affected by miR-210 gene silencing was at the $p < 0.05$ (*) significance level. Therefore, the silencing effect of miR-210 has a far more targeted effect than HIF-1α suppression, because other members of the HIF family (HIF-2, -3) also affect miR-210[35-37].

Detection of HIF-1α and MiRNA-210 Expression Level

Cells affected by HIF-1α and miR-210 gene silencing showed no significant changes in the expression level of the genes of interest in normoxia, whereas in hypoxia they did (Figure 2-B-1, 2). The gene expression in cells in normoxia after gene silencing had lower levels of HIF-1α mRNA expression compared to the NTC group. In the hypoxic environment, the detection of HIF-1α mRNA in miR-210 silent cells was done by increased expression of HIF-1α which is sufficient due to induced hypoxia.

Cells with HIF-1α gene silencing were characterised by the highest level of miR-210 expression which correlates with the present hypoxia because miR-210 and HIF-1α, as well as HIF-2, -3, interact and cooperate[35-37].

Cell Viability in Normo- and Hypoxic Conditions

The level of intracellular (cytosolic) NADH increases by activating the apoptotic process in the cell, while at the same time the concentration of free NADH in the mitochondrial matrix decreases continuously, thereby reducing ATP formation, increasing ROS levels, leading to self-destruction by apoptosis, necrosis or necrotic apoptosis[38-40]. Under normal conditions NADH is accumulated in the mitochondria[41].

Oxygen Consumption Rate

Oxygen Consumption Rate (OCR) describes the level of oxygen value consumed by cells in

the time. OCR is the key indicator of mitochondrial respiration and its metabolic function. An increase in the basal respiration was observed for both cells cultured in normo- or hypoxic conditions with glucose (Glc), as well as glutamine (Gln) NTC, HIF-1α and miR-210.

Mitochondrial viability under both normoxic and hypoxic conditions was almost zero for cells cultured with 10 mM Glc, as well as with 10 mM Gln in the culture medium (Figure 3-A-1, 2). Thus, energy for cells was obtained by increasing the activity of glycolysis in the cytosol, which compensated for the lack of energy from the OXPHOS pathway.

The observed changes in mitochondrial viability result from activation of proton and electron transfer by respiratory complexes resulting in energy production by ATP synthase. MM cells are predominantly glycolytic (cytosolic) in both normoxia and hypoxia since respiratory complexes are unable to transfer protons and electrons. By HIF-1α and miR-210 gene silencing, the effect of hypoxia on protein transporters was inhibited, leading to increased mitochondrial activity in both normoxic and hypoxic conditions.

It is known that cancer cells acquire energy from non-glucose precursors, e.g., glutamine, and use them more efficiently[42]. Glutamine is an anaplerotic intermediate in the citrate cycle in the formation of the 2-oxoglutarate; however, no effect in NTC measurements was observed. These results suggest the utilisation of glutamine in tumour cells *via* reductive carboxylation.

This work demonstrates that gene silencing of hypoxia transcription factors has a positive feedback in mitochondrial activity in normoxia, as well as in hypoxia condition. We observed several benefits of gene silencing of HIF-1α, and miR-210 as increase ATP production, stimulation of mitochondrial biogenesis, and presumably also pro-apoptic signals. This suggests that the gene silencing of HIF-1α even miR-210 is involved in the TCA cycle (HIF-1α silencing), electron transport chain in respiratory complexes (miR-210 silencing), and could increase mitochondrial mass (because of increased maximal respiratory capacity), or mitochondrial membrane potential (because of increased proton leak). This effect is more putative for cancer cells in high cancer stage, which is described by glutaminolysis. Our results suggest the same, if not better, beneficial effect of miR-210 silencing on MM cells fed with glutamine.

Conclusions

The aim of the present study was to elucidate the effect of hypoxia (or mimic hypoxia) on the energetic metabolic changes of malignant melanoma cells. At the same time, respiration efficiency and the NADH/NAD^+ production ratio in MM cell lines were analysed.

The study concludes that malignant melanoma cells under normoxic and hypoxic conditions show significantly less accumulation of NADH after gene silencing of hypoxic transcription factors. This phenomenon was even more pronounced upon a replacement of glucose with glutamine as the main substrate in cultivation media.

This reduction in the accumulation of NADH in the cytosol was reflected in the acceleration of mitochondrial metabolism in normoxia/hypoxia in both glucose-fed and glutamine-fed cells. Cells not affected by gene silencing showed no significant mitochondrial activity and energy metabolism was mainly aimed in the cytosol resulting in a high level of NADH in normoxia, and especially in hypoxia as described by the well-known Warburg effect.

Reactivation of mitochondrial metabolism in malignant melanoma cells leads to their reduced viability and possibly apoptotic processes. Our findings suggest the potential use of targeted HIF-1α, and miR-210 respectively gene silencing in therapy of malignant melanoma.

Conflict of Interests

The Authors declare that they have no conflict of interests.

References

1) Zheing J. Energy metabolism of cancer: glycolysis versus oxidative phosphorylation. Oncol Lett 2012; 4: 1151-1157.
2) Solaini G, Sgarbi G, Baracca A. Oxidative phosphorylation in cancer cells. BBA – Bioenergetics 2011; 1807: 534-542.
3) Loftus SK, Baxter LL, Cronin JC, Fufa TD, NISC Comparative Sequencing Program, Pavan WJ. Hypoxia-induced HIF1α targets in melanocytes reveal a molecular profile associated with poor melanoma prognosis. Pigment Cell Melanoma Res 2017; 30: 339-352.
4) Karuppagounder S, Ratan RR. Hypoxia-inducible factor prolyl hydroxylase inhibition: robust new target or another bigbust for stroke therapeutics? J Cereb Blood Flow Metab. 2012; 32: 1347-1361.

5) Cortez MA, Ivan C, Zhou P, Wu X, Ivan M, Calin GA. MicroRNAs in cancer: from bench to bedside. Adv Cancer Res 2010; 108: 133-157.

6) Anton L, DeVine A, Polyak E, Olarerin-George A, Brown, Falk MJ, Elovitz MA. HIF-1α stabilization increases miR-210 eliciting first trimester extravillous trophoblast mitochondrial dysfunction. Front Physiol 2019; 10: 699.

7) Chan SY, Zhang YY, Hemann C, Mahoney CE, Zweier J, Loscalzo J. MicroRNA-210 controls mitochondrial metabolism during hypoxia by repressing the iron-sulfur cluster assembly proteins ISCU1/2. Cell Metab 2009; 10: 273-284.

8) Chen Z, Li Y, Zhang H, Huang P, Luthra R. Hypoxia-regulated microRNA-210 modulates mitochondrial function and decreases ISCU and COX10 expression. Oncogene 2010; 29: 4362-4368.

9) Bavelloni A, Ramazzotti G, Poli A, Piazzi M, Focaccia E, Blalock W, Faenza I. MiRNA-210: a current overview. Anticancer Res 2017; 37: 6511-6521.

10) Loh HY, Norman BP, Lai KS, Rahman NMANA, Alithreen NBM, Osman MA. The regulatory role of microRNAs in breast cancer. Int J Mol Sci 2019; 20: 4940.

11) Bartoszewska S, Janaszak-Jasiecka A, Ochocka RJ, Collawn JF, Bartoszewski R. miRNAs regulate the HIF switch during hypoxia: a novel therapeutic target. Angiogenesis 2018; 21: 183-202.

12) Cherradi N. microRNAs as potential biomarkers in adrenocortical cancer: progress and challenges. Front Endocrinol 2016; 6: 195.

13) He R, Cen W, Cen J, Cen W, Li JY, Li MW, Gan TQ, Hi XH, Chen G. Clinical Significance of miR-210 and its prospective signaling pathways in non-small cell lung cancer: evidence from gene expression omnibus and the cancer genome atlas data mining with 2763 samples and validation via real-time quantitative PCR. Cell Physiol Biochem 2018; 46: 925-952.

14) Puisségur MP, Mazure NM, Bertero T, Pradelli L, Grosso S, Robbe-Sermesant K, Maurin T, Lebrigand K, Cardinaud B, Hofman V, Fourre S, Magnone V, Ricci JE, Pouysségur J, Gounon P, Hofman P, Barbry P, Mari B. MiR-210 is overexpressed in late stages of lung cancer and mediates mitochondrial alterations associated with modulation of HIF-1 activity. Cell Death Differ 2011; 18: 465-478.

15) McGarty TP. Warburg and prostate cancer. 2018; [online] Available at: http://www.telmarc.com/Documents/White%20Papers/149Warburg2.pdf

16) Benita Y, Kikuchi H, Smith AD, Zhang MQ, Chung DC, Xavier RJ. An integrative genomics approach identifies Hypoxia Inducible Factor-1 (HIF-1)-target genes that form the core response to hypoxia. Nucleic Acids Res 2009; 37: 4587-4602.

17) Yang OCY, Maxwell PH, Pollard PJ. Renal cell carcinoma: translational aspects of metabolism and therapeutic consequences. Kidney Int 2013; 84: 667-681.

18) Cantó C, Menzies K, Auwerx J. NAD(+) metabolism and the control of energy homeostasis - a balancing act between mitochondria and the nucleus. Cell Metab 2015; 22: 31-53.

19) Matés JM, Di Paola FJ, Campos-Sandoval JA, Mazurek S, Márquez J. Therapeutic targeting of glutaminolysis as an essential strategy to combat cancer. Semin Cell Dev Biol 2019; S1084-9521: 30073-30074.

20) Choi YK, Park KG. Targeting glutamine metabolism for cancer treatment. Biomol Ther 2018; 26: 19-28.

21) Alberghina L, Gaglio D. Redox control of glutamine utilization in cancer. Cell Death Dis 2014; 5: e1561.

22) Yoshida GJ. Metabolic reprogramming: the emerging concept and associated therapeutic strategies. J Exp Clin Cancer Res 2015; 34: 111.

23) Natarajan SK, Venneti S. Glutamine metabolism in brain tumors. Cancers (Basel) 2019;11. pii: E1628.

24) Nguyen TL, Durán RV. Glutamine metabolism in cancer therapy. Cancer Drug Resist 2018; 1: 126-138.

25) Ma Y, Temkin SM, Hawkridge AM, Guo C, Wang W, Wang XY, Fang X. Fatty acid oxidation: an emerging facet of metabolic transformation in cancer. Cancer Lett 2018; 435: 92-100.

26) Jin L, Alesi GN, Kang S. Glutaminolysis as a target for cancer therapy. Oncogene 2016; 35: 3619-3625.

27) Elguindy MM, Nakamaru-Ogiso E. Apoptosis-inducing Factor (AIF) and its family member protein, AMID, are rotenone-sensitive NADH: ubiquinone oxidoreductases (NDH-2). J Biol Chem 2015; 290: 20815-20826.

28) Sun F, Dai Ch, Xie J, Hu X. Biochemical issues in estimation of cytosolic free NAD/NADH ratio. PLoS One 2012; 7: e34525.

29) Li Q, Ma R, Zhang M. CoCl2 increases the expression of hypoxic markers HIF-1α, VEGF and CXCR4 in breast cancer MCF-7 cells. Oncol Lett 2018; 15: 1119-1124.

30) Hung YP, Yellen G. Live cell imaging of cytosolic NADH-NAD+ redox state using a genetically encoded fluorescent biosensor. Methods Mol Biol 2014; 1071: 83-95.

31) Forrest MD. NADH as a cancer medicine. bioRxiv 2015; 019307.

32) Walenta S, Muller-Klieser WF. Lactate: mirror and motor of tumor malignancy. Semin Radiat Oncol 2004; 14: 267-274.

33) Filipp FV, Scott DA, Ronai ZA, Osterman AL, Smith JW. Reverse TCA cycle flux through isocitrate dehydrogenases 1 and 2 is required for lipogenesis in hypoxic melanoma cells. Pigment Cell Melanoma Res 2012; 25: 375-383.

34) Fasanaro P, Greco S, Lorenzi M, Pescatori M, Brioschi M, Kulshreshtha R, Banfi C, Stubbs A, Calin GA, Ivan M, Capogrossi MC, Martelli F. An integrated approach for experimental target identification of hypoxia-induced miR-210. J Biol Chem 2009; 284: 35134-35143.

35) Chan YC, Banerjee J, Choi SY, Sen ChK. MiR-210: the master hypoxamir. Microcirculation 2012; 19: 215-223.

36) McCormick RI, Blick C, Ragoussis J, Schoedel J, Mole DR, Young AC, Selby PJ, Banks RE, Harris AL. MiR-210 is a target of hypoxia-inducible factors 1 and 2 in renal cancer, regulates ISCU and correlates with good prognosis. Brit J Cancer 2013; 108: 1133-1142.

37) Serocki M, Bartoszewska S, Janaszak-Jasiecka A, Ochocka RJ, Collawn JF, Bartoszewski R. MiRNAs regulate the HIF switch during hypoxia: a novel therapeutic target. Angiogenesis 2018; 21: 183-202.

38) Su J, Liu J, Yan XY, Zhang Y, Zhang JJ, Zhang LC, Sun LK. Cytoprotective effect of the UCP2-SIRT3 signaling pathway by decreasing mitochondrial oxidative stress on cerebral ischemia-reperfusion injury. Int J Mol Sci 2017; 18. pii: E1599.

39) Brohem CA, Massaro RR, Tiago M, Marinho CE, Jasiulionis MG, de Almeida RL, Rivelli DP, Albuquerque RC, de Oliveira TF, de Melo Loureiro AP, Okada S, Soengas MS, de Moraes Barros SB, Maria-Engler SS. Proteasome inhibition and ROS generation by 4-nerolidylcatechol induces melanoma cell death. Pigment Cell Melanoma Res 2012;25: 354-369.

40) Voľavská M. Oxidative stress and endothelial dysfunction in atherosclerosis. Ateroskleróza: metabolizmus, klinika, liečba 2006; 10: 48-55.

41) Wang X, Li H, Ding S. The effects of NAD+ on apoptotic neuronal death and mitochondrial biogenesis and function after glutamate excitotoxicity. Int J Mol Sci 2014; 15: 20449-20468.

42) Cruzat V, Macedo Rogero M, Noel Keane K, Curi R, Newsholme P. Glutamine: metabolism and immune function, supplementation and clinical translation. Nutrients 2018; 10. pii: E1564.